AIAA 97-2200
Assessment of Store Control Surface Effectiveness in a Non-uniform Aircraft Flow Field

R. H. Nichols and S. B. Evans
Sverdrup Technology, Inc., AEDC Group
Arnold Engineering Development Center
Arnold Air Force Base, Tennessee 37389

15th Applied Aerodynamics Conference
June 23 - 25, 1997 / Atlanta, GA

ASSESSMENT OF STORE CONTROL SURFACE EFFECTIVENESS IN A NON-UNIFORM AIRCRAFT FLOW FIELD*

*R. H. Nichols** and S. B. Evans†*
Sverdrup Technology, Inc., AEDC Group
Arnold Engineering Development Center
Arnold Air Force Base, TN 37389

Abstract

Comparisons of the control effectiveness for two stores in free stream and in the flow field of a parent aircraft have been performed using computational fluid dynamics (CFD). The computations were performed to assess the changes in control surface effectiveness of the store due to the highly nonlinear flow field of the parent aircraft at transonic speeds. The Navier-Stokes equations were solved using an algebraic turbulence model for an extended range air-to-ground missile (AGM-130A) mounted on the wing pylon of an F-15E aircraft and for an air-to-air missile mounted on the forward station of the inboard pylon of an F-15E aircraft. Free-stream calculations showed good agreement with wind tunnel control surface effectiveness results for both stores. Calculations of control surface effectiveness in the aircraft flow field indicate significant changes occur for the AGM-130A missile while the air-to-air missile showed very little effect. This is attributed to the fact that a large region of separated flow occurs on the lee side of the deflected flap of the AGM-130A while the flow over the air-to-air missile deflected elevator is attached.

Nomenclature

C	Local chord length at a spanwise position
CA	Missile axial-force coefficient
CN	Missile normal-force coefficient
CY	Missile side-force coefficient
Cp	Pressure coefficient
cl	Missile rolling-moment coefficient
cm	Missile pitching-moment coefficient
cn	Missile yawing-moment coefficient
L	Length of missile centerbody
M	Mach number
P	Static pressure
PINF	Free-stream static pressure
rcx	Ratio of carriage to free-stream control surface-induced incremental axial-force coefficients
rcy	Ratio of carriage to free-stream control surface-induced incremental side-force coefficients
rcz	Ratio of carriage to free-stream control surface-induced incremental normal-force coefficients
rmx	Ratio of carriage to free-stream control surface-induced incremental rolling-moment coefficients
rmy	Ratio of carriage to free-stream control surface-induced incremental pitching-moment coefficients
rmz	Ratio of carriage to free-stream control surface-induced incremental yawing-moment coefficients
X	Coordinate axis, positive rearward as viewed by the pilot
u_τ	Wall friction velocity
y^+	Nondimensional distance from the wall ($\rho_{wall} y_n u_\tau / \mu_{wall}$)
y_n	Normal distance from wall
Δ	Force or moment increment
δ_i	Control surface deflection angle

* The research reported herein was performed by the Arnold Engineering Development Center (AEDC), Air Force Materiel Command. Work and analysis for this research were performed by personnel of Sverdrup Technology, Inc., AEDC Group, technical services contractor for AEDC. Further reproduction is authorized to satisfy needs of the U. S. Government.

** Senior Member, AIAA.

† Member, AIAA.

μ Molecular viscosity

ρ Density

Introduction

Separation of stores from a parent aircraft at transonic speeds can be a difficult problem because of the highly nonlinear nature of the flow field between the two bodies. The difficulty of the problem is increased when the store is required to maneuver in this highly nonlinear flow field. Wind tunnel data for control surface effectiveness of a weapon in the presence of an aircraft has not been obtained in the past because of the expense and complexity of the models required to acquire the data. Current engineering models assume that free-stream control effectiveness wind tunnel data can be used for trajectory simulation when the weapon is in the vicinity of the parent aircraft. The purpose of this study is to investigate the validity of this assumption using computational fluid dynamics (CFD), and to suggest possible means of improving the accuracy of current engineering models of control surface effectiveness when the store is in the aircraft flow field.

CFD is not limited by the constraints of model complexity, scale, and support requirements that plague the wind tunnel when testing aerodynamic bodies in close proximity. The ability of CFD to accurately predict the loads and trajectories of stores in the flow field of a parent aircraft has been demonstrated by a number of investigators including Fox, et al.,[1] Donegan and Fox,[2] and Nichols, et al.[3] These studies indicate that CFD can provide meaningful insight into complex multi-body problems if care is taken to include the appropriate physical processes and geometrical detail. CFD also allows the analyst to look at the details of the flow field, adding insight that cannot be obtained from traditional wind tunnel tests.

Configuration

Two store geometries were investigated in this study. The first geometry is an extended range air-to-ground missile (AGM-130A) shown in Fig. 1. The second geometry is an air-to-air missile shown in Fig. 2. These two stores were chosen because of the extensive wind tunnel database available for each store and because they represent two classes of maneuvering stores common in the current Air Force inventory: a weapon with a wing-flap arrangement and a weapon with an all-moving aft control surface.

The F-15E aircraft configuration used with the AGM-130A missile included:

1. F-15E aircraft with conformal fuel tanks (CFT), standard pylons, and ingesting inlets.
2. Four AIM-7F missiles on the CFT inboard long pylons (two missiles on each side of the aircraft).
3. Centerline data-link pod.
4. LANTIRN pods.
5. AGM-130A missiles on the inboard wing pylons.

The F-15E configuration used with the air-to-air missile included:

1. F-15E aircraft with conformal fuel tanks (CFT), standard pylons, and ingesting inlets.
2. LANTIRN pods.
3. Air-to-air missiles on the forward station of the inboard long pylon.

The flight condition used with the AGM-130A missile was a Mach number of 0.85, an aircraft angle of attack of 2 deg, and a full-scale Reynolds number of 0.5 million per foot. The free-stream calculations for the AGM-130A missile were per-

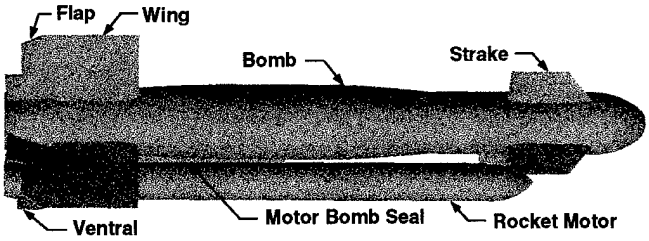

Fig. 1. AGM-130A geometry (flap 3 deflected).

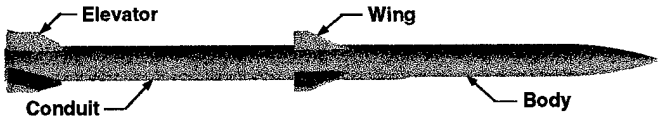

Fig. 2. air-to-air missile geometry (elevators 2 and 4 deflected).

formed with a missile angle of attack of 1.5 deg, which corresponds to the angular orientation of the missile in the carriage position on the wing pylon of the F-15E aircraft when the aircraft is at 2-deg angle of attack. The flight condition used with the air-to-air missile was a Mach number of 0.9, an aircraft angle of attack of 0 deg, and a full-scale Reynolds number of 0.66 million per foot. The free-stream calculations for the air-to-air missile were performed with a missile angle of attack of 0 deg.

Approach

The CFD analysis effort required that force- and moment- coefficient increments between deflected control surface and undeflected control surface configurations and between free-stream and aircraft interference flow fields be calculated. Experience has shown that when loads on a vehicle in different flow conditions are computed, the results are more accurate when the computational grids for the vehicle are the same for all cases. This eliminates biases in the solutions from differences in the grids. Based on this observation, the chimera overset grid methodology[4] was used. The chimera overset grid methodology allows grids for each component (i.e., a strake, wing, flap, or body) of each vehicle to be generated separately and then brought together by communication through interpolated boundaries. This intergrid communication is established by the PEGSUS[5] code.

The 3D Euler and Navier-Stokes equations were solved using the implicit, approximate factorization scheme of Beam and Warming.[6] The coded form of the scheme is a vectorized enhancement of the version developed by Pulliam and Steger.[7] The second- and fourth-order implicit and explicit smoothers of Benek, et al.[8] were used to suppress oscillations and improve stability of the central-difference algorithm. The Baldwin-Lomax[9] algebraic turbulence model was used in this study.

All boundaries were updated explicitly. The far-field boundaries were frozen at free-stream values. Simple extrapolation of all conserved variables was used on the downstream outflow boundary. Tangent-flow wall conditions were used on all F-15E, AIM-7F, and data pod solid surfaces. No-slip boundary conditions were imposed on all AGM-130A and air-to-air missile solid surfaces. The F-15E inlet mass-flow rate was controlled by placing a choked nozzle grid at the exit of the inlet grid. The throat area was sized to provide a full-scale corrected mass-flow rate of 225 lbm/sec.

Twenty-three grids with approximately 3 million points were used to discretize the AGM-130A missile. The gap between the missile wings and the flaps and the gaps between the missile flaps and the missile body were included for all flaps. Each flap was individually discretized so that any flap deflection combination could be simulated by simply rotating the flap grids about their hinge lines with the chimera methodology. Each flap mesh contained 170,569 points. Only flap 3 was deflected in this study. The lugs and the cable tray were not included in this study. The grid spacing at the wall corresponded to a y^+ of five for all solid surfaces. An additional "outer" mesh was used in the free-stream calculations to move the computational free-stream boundaries out to approximately ten missile diameters from the body.

The air-to-air missile was discretized using eleven grids with approximately 2 million points. The missile aft control surfaces (elevators) were individually discretized so that they could be deflected in any combination by simply rotating the elevator grids about their hinge lines utilizing the chimera methodology. The gap between the control surfaces and the missile body was included for all control surfaces in this study. Each elevator contained 137,385 points. Elevators 2 and 4 were deflected in this study. The lugs were not included. The grid spacing at the wall corresponded to a y^+ of five for all solid surfaces. An additional "outer" mesh was used in the free-stream calculations to move the computational free-stream boundaries out to approximately 40 missile diameters from the body.

A half-model computational discretization of the F-15E aircraft with symmetry boundary conditions was used in this study. Donegan and Fox[2] indicated that outwash due to inlet spillage had significant effect on the loads and trajectories of stores mounted on the forward station of the inboard long pylon. Because of this, care was taken to model the inlet and diverter in detail. The basic aircraft, pylons, and LANTIRN pods comprised a grid sys-

tem which included 19 grids with approximately 0.95 million points. The aircraft horizontal and vertical tails and nozzle-afterbody region were not modeled. The AIM-7F missiles and the data pod grids were added for the AGM-130A calculations. These grids added an additional 0.3 million points. The F-15E aircraft, AIM-7F missiles, and the data pod were all modeled with inviscid grids.

Force- and moment-coefficients on the missiles were determined from integration of the surface pressures using the TESS[10] code. TESS was developed to allow forces to be calculated on overlapping surfaces by using Delauney triangulation of the points in the overlapped region. TESS also allows the forces to be calculated on separate components of a complicated body so that the contribution of each component may be analyzed.

Results

Calculations were performed for both stores in free stream and in the carriage position on the F-15E aircraft. Force- and moment-coefficient increments between the deflected control surface and undeflected control surface configurations were obtained for each store in free stream and at carriage. The increments are defined as the total force or moment coefficient on the store with control surface deflected minus the total force or moment coefficient on the store with no control surface deflection. Calculations were also performed on the F-15E aircraft without the store to characterize the flow field in which the store would be placed.

AGM-130A

Free-Stream Results — Free-stream computations were performed for the AGM-130A missile with flap 3 (the lower-inboard flap when the missile is located on the aircraft right wing pylon) deflected 0, –10, and –20 deg (trailing edge up). The pressure-coefficient contours on the missile with flap 3 deflected –20 deg are shown in Fig. 3. The results presented in Fig. 3 are for the missile at the carriage position on the aircraft, but the contours show the same features as the missile in free stream. Note the high-pressure region on the body due to the flow about the windward side of the deflected flap. The force- and moment-coefficient incremental results are in excellent agreement with wind tunnel data obtained at AEDC[4] as shown in Fig. 4. Also shown are results from Euler calculations. The Euler results significantly overpredict the flap effectiveness. Figure 5 shows velocity vectors at the quarter-span location of flap 3 for both the –10 and

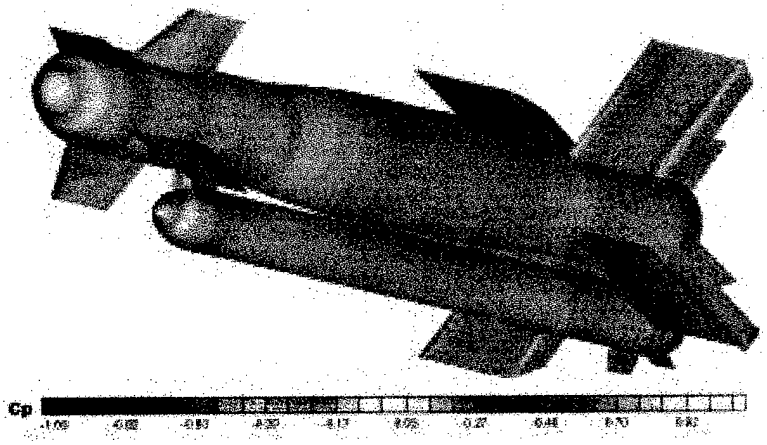

Fig. 3. Pressure coefficient contours for the AGM-130A for M = 0.85, α = 1.5 deg, and δ_3 = –20 deg.

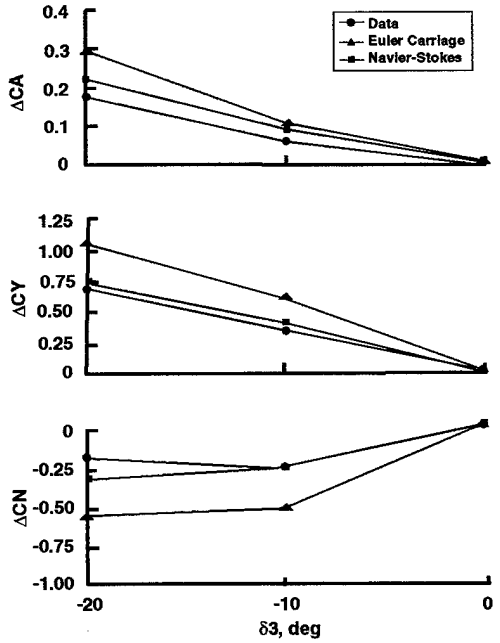

Fig. 4. Free-stream force- and moment-incremental coefficients for the AGM-130A for M = 0.85 and α = 1.5 deg.

–20 deg deflections. Note that the hinge line is not at the leading edge of the flap, producing a complicated 3D flow pattern at the flap leading edge and in the wing-flap gap region. Both flap deflections have a separated flow region near the leading edge due to the wake of the wing. Further back on the leeward side of the flap, a separation region can be seen which increases with size with increasing flap deflection. The differences between the Euler predictions and the data are attributable to the presence of the large region of separated flow.

With the large amount of separated flow present on the flap, the flap force- and moment-increments would be expected to be nonlinear functions of the flap deflection angle, with a plateau and/or a roll-off beginning at the flap deflection angle where separation of the flow occurs. The normal- force and the pitching-moment increments are not linear with flap deflection, while the side-force and yawing-moment increments are almost linear over the range of flap deflection angles investigated. This is because of an aerodynamic interaction between the missile body and the deflected flap as can be seen by the loads on the body alone and the deflected flap alone with varying flap deflection as shown in Fig. 6. The aerodynamic interaction tends to augment the side-force

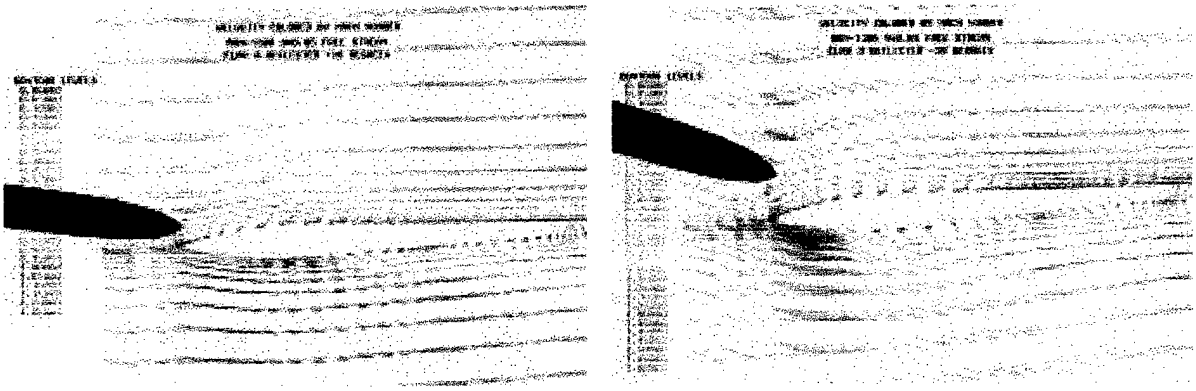

a. Flap deflected –10 deg b. Flap deflected –20 deg

Fig. 5. Velocity vectors at the 0.25 spanwise location of flap 3 deflected for AGM-130A in free stream.

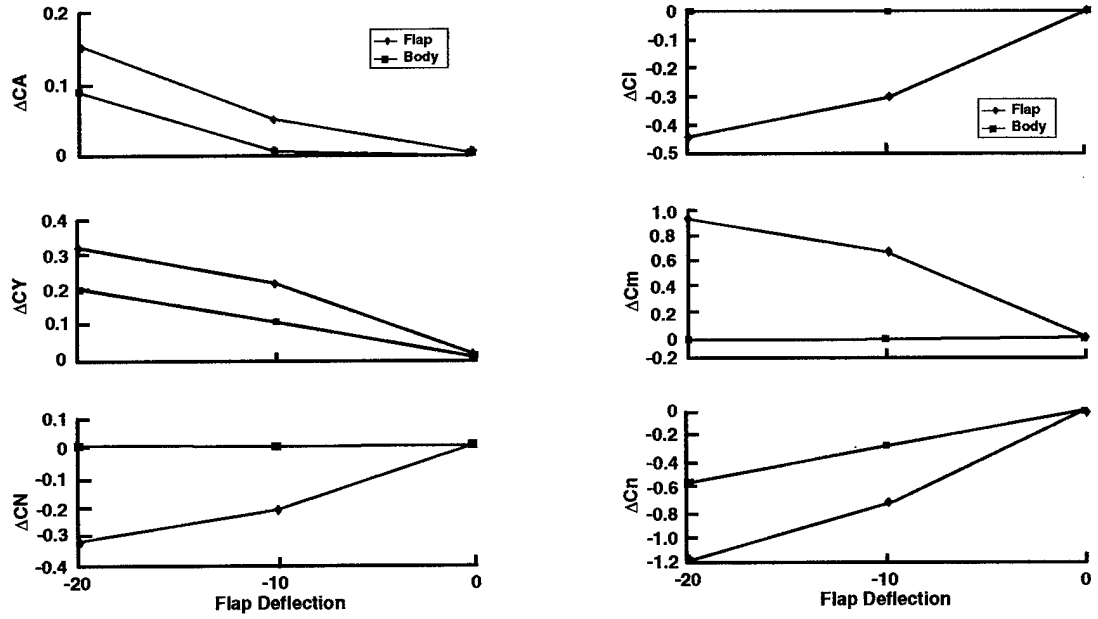

Fig. 6. Free-stream force and moment incremental contributions of the deflected flap and the body for the AGM-130A for M = 0.85 and α = 1.5 deg.

and yawing-moment increments and produce the almost linear behavior of these coefficients. The augmentation seems to be driven by the windward side of the deflected flap, so that forces and moments in only one direction are affected.

F-15E Flow Field without AGM-130A — Calculations were performed for the F-15E aircraft at a Mach number of 0.85 and an angle of attack of 2 deg without the AGM-130A missile present on the wing pylon. The centerline data pod and the AIM-7F missiles were included in this calculation. The Mach number and flow-angle distributions along the centerline of the centerbody of the AGM-130A missile (as if the missile were at carriage) are shown in Figs. 7 and 8. The Mach number is seen to be higher than free stream over the entire length of the centerbody. The variation in Mach number along the centerbody length is only about 0.05, and the mean value is about 0.89. The crossflow along the centerbody is seen to cause a couple which will cause the missile to rotate with the nose away from the aircraft immediately upon separation. The magnitude of the flow angles is relatively small.

F-15E Flow Field with AGM-130A — Calculations with the AGM-130A in the carriage position on the F-15E aircraft were then performed. The pressure coefficient contours with the AGM-130A flap 3 deflected –20 deg are shown in Fig. 9. The force- and moment-coefficient increments are shown in Fig. 10. Also included are computational results using the Euler equations and the Navier-Stokes free-stream computational results. Large differences between the carriage and the free-stream results are seen in all coefficients. The incremental force- and moment-coefficients due to flap 3 alone and the body alone are shown in Fig. 11. The flap contribution is seen to be approximately half of the free-stream results shown in Fig. 6. The augmentation of the side force and the yawing moment due to the aerodynamic interaction between the body and the flap is slightly affected by the flow field at carriage. An unfavorable aerodynamic interaction on the body in normal force and pitching moment is seen at carriage that did not exist in free stream. The ratio of the force- and moment-coefficient increments from carriage

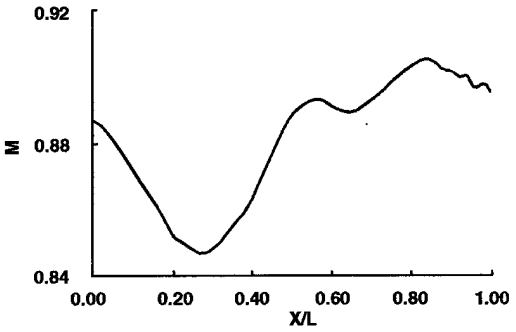

Fig. 7. Mach number distribution at the AGM-130A centerbody axis location at carriage position in the F-15E flow field (missile not present) for M = 0.85 and α = 2 deg.

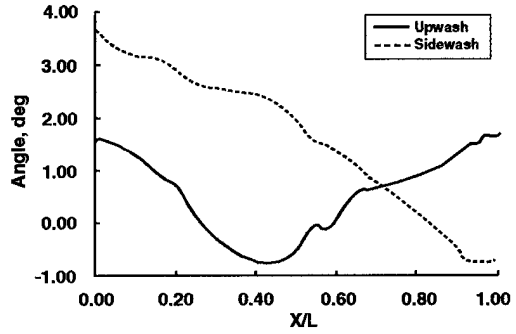

Fig. 8. Flow angle distribution at the AGM-130A centerbody axis location at carriage position in the F-15E flow field (missile not present) for M = 0.85 and α = 2 deg.

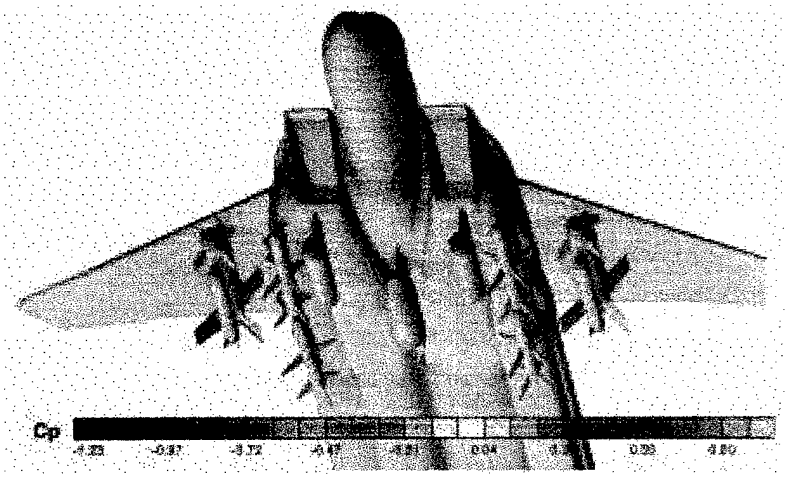

Fig. 9. Pressure coefficient contours for the F-15E with the AGM-130A at carriage for M = 0.85, α = 2 deg, and δ_3 = –20 deg.

to free stream is shown in Table 1. The losses in flap effectiveness are clearly seen.

The pressure-coefficient distributions on flap 3 for 0-, –10-, and –20-deg deflections at two spanwise locations are shown in Fig. 12 for the missile at both free stream and carriage. The loss in force from free stream to carriage generated by the flap can be clearly seen. The largest losses seem to occur near the leading edge of the flap. There is a significant loss in pressure on the leeward side of the flap, which is consistent with an upstream

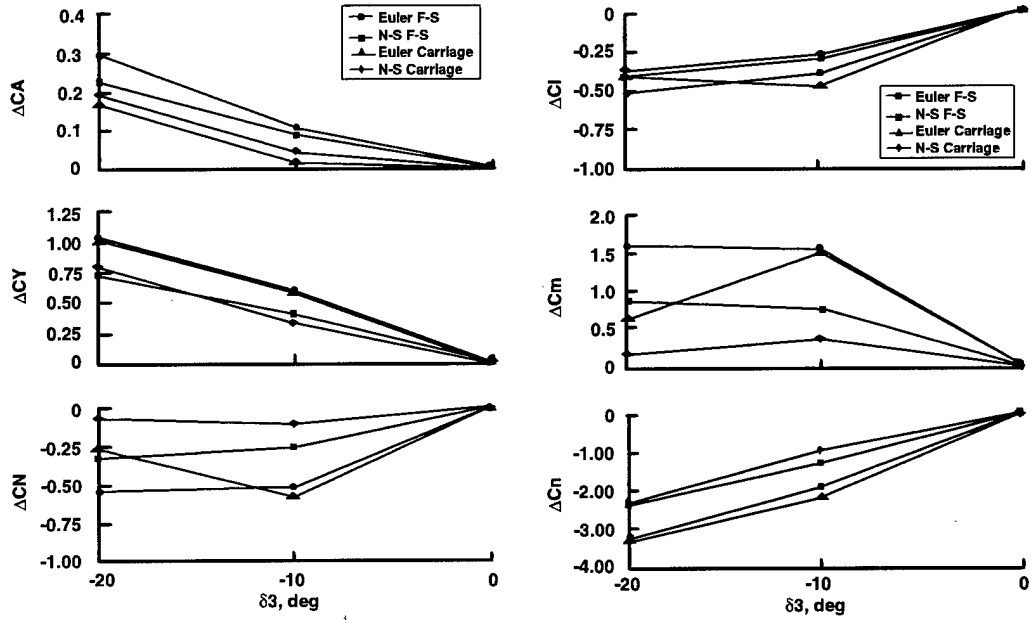

Fig. 10. Force and moment incremental contributions for the AGM-130A at carriage and in free stream for M = 0.85.

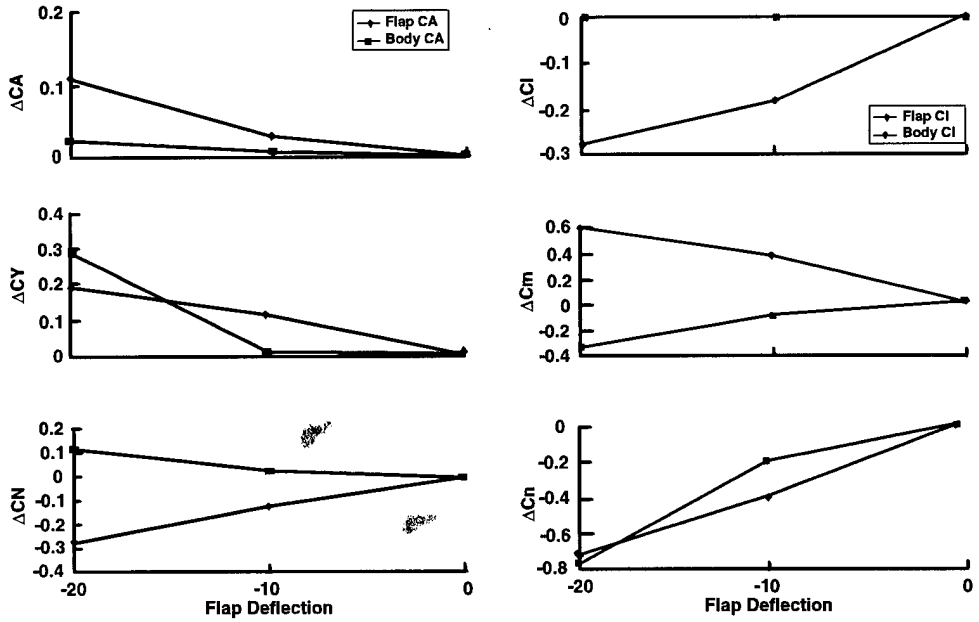

Fig. 11. Carriage force- and moment-coefficient incremental contributions for the AGM-130A at carriage and in free stream for M = 0.85.

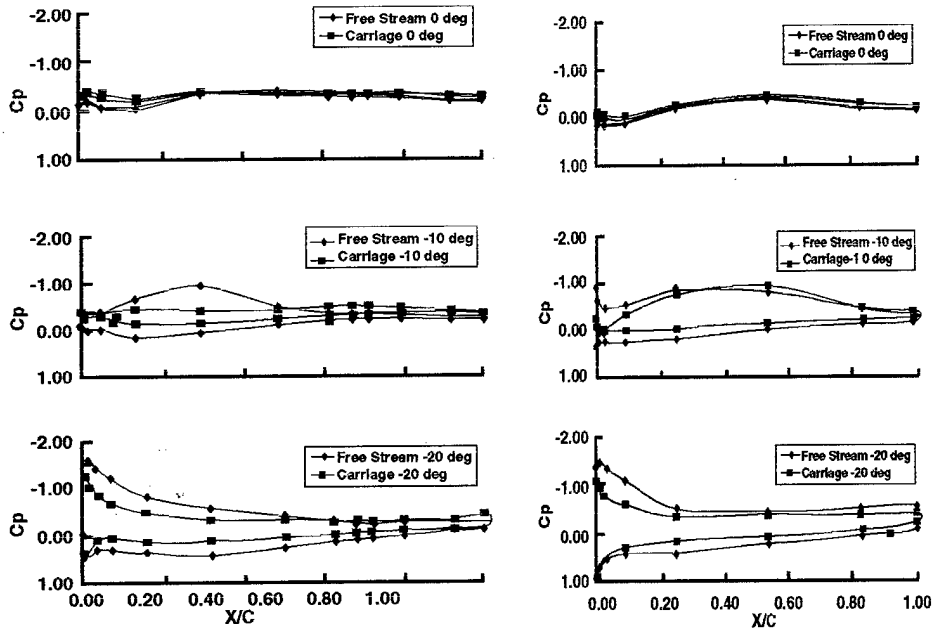

Fig. 12. Pressure coefficient distributions on the deflected flap of the AGM-130A for M = 0.85.

Table 1. CFD predicted ratio of force- and moment-coefficient increments at the carriage position to the free-stream force- and moment-coefficient increments

	δ_3, deg	rcx	rcy	rcz	rmx	rmy	rmz
Euler	–10	0.1215	1.0145	1.1241	1.2040	0.9596	1.1413
N-S	–10	0.4765	0.7203	0.4273	0.8871	0.4550	0.7088
Euler	–20	0.5835	0.9943	0.5144	0.7880	0.3836	1.0123
N-S	–20	0.8888	1.1600	0.0960	1.1482	0.1160	1.0634

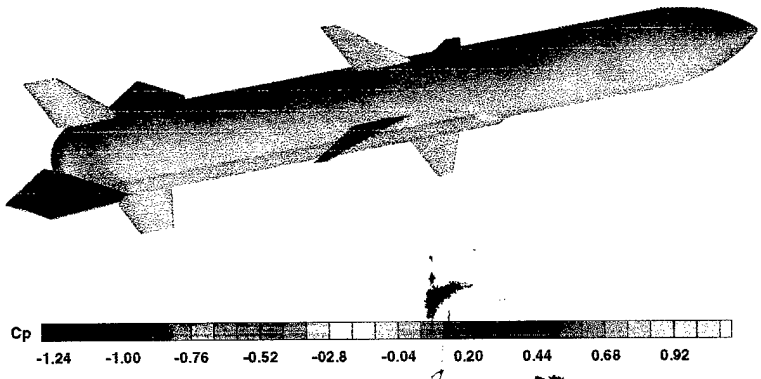

Fig. 13. Pressure coefficient contours for the air-to-air missile for M = 0.9, α = 0 deg, and $\delta_{2,4}$ = –20 deg.

movement of the transonic shock on the flap. The presence of the large region of separated flow on the leeward side of the flap increases the sensitivity of the local flow field to the presence of the aircraft.

Air-to-air Missile Results

Free-Stream Results — Free-stream calculations for the air-to-air missile with elevators 2 and 4 deflected 0, –10, and –20 deg (trailing edge up with the missile oriented with elevators 2 and 4 in the horizontal plane) were performed. Pressure-coefficient contours with elevators 2 and 4 deflected –20 deg are shown in Fig. 13. The results shown in Fig. 13 are for the missile in the carriage position on the aircraft, but the contours show the same features as the free-stream case. There is a large interaction region between the deflected elevator and the body, as is indicated by the region of high pressure on the body due to the flow about the windward side of the deflected elevator. Force- and moment-coefficient increments are shown with experimental data[5] in Fig. 14. There is excellent agreement between CFD and experiment for all coefficients. Note the differ-

ences in scale for the pitching- and yawing-moment results. The coefficients are nearly linear over the range of elevator deflection investigated. Velocity vectors are shown for the midspan location of elevator 4 deflected –20 deg in Fig. 15. The flow is seen to be attached at all stations, although separation of the boundary layer appears imminent on the leeward side near the leading edge.

F-15E Flow Field without Air-to-air Missile — The F-15E aircraft flow field was calculated without the air-to-air missile present. The Mach number and flow angle distributions along the missile centerline as if the missile were in the flow field are shown in Figs. 16 and 17. Significant excursions for free-stream values are seen along the body axis. The Mach number varies from 0.8 to 1.2 along the body. Large values of upwash and sidewash are also seen to exist. The flow field caused the missile to yaw with the nose away from the aircraft and to pitch down upon release from the aircraft.

F-15E Flow Field with Air-to-air Missile — Calculations were performed with the missile in the

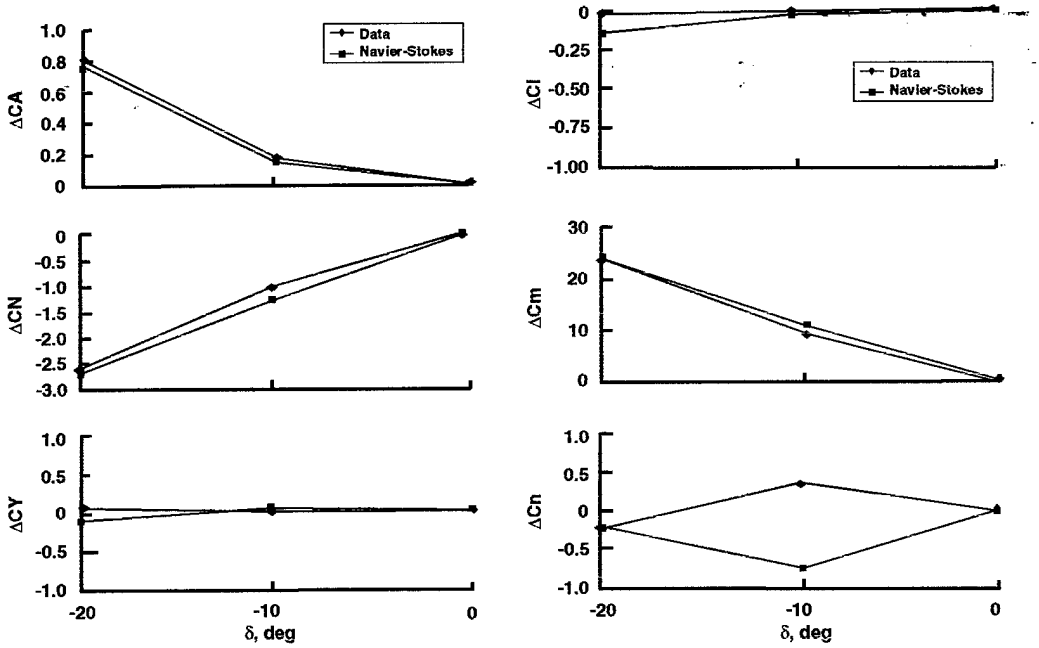

Fig. 14. Free-stream force and moment incremental coefficients for the air-to-air missile for M = 0.9 and α = 0 deg.

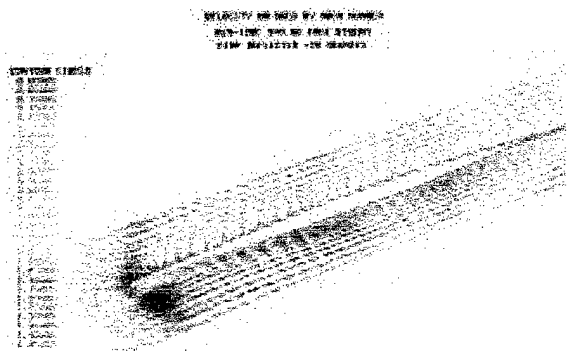

Fig. 15. Velocity vectors at the 0.5 spanwise location of elevator 2 deflected –20 deg for the air-to-air missile in free stream.

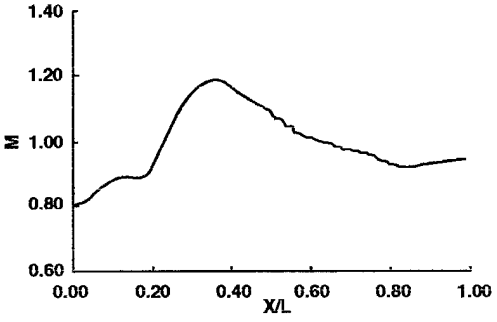

Fig. 16. Mach number distribution at the air-to-air missile centerbody axis location at carriage position in the F-15E flow field (missile not present) for M = 0.9 and α = 0 deg.

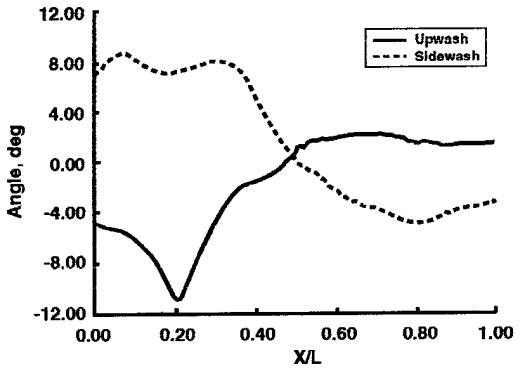

Fig. 17. Flow angle distribution at the air-to-air missile centerbody axis location at carriage position in the F-15E flow field (missile not present) for M = 0.9 and α = 0 deg.

aircraft flow field. Pressure-coefficient contours for the aircraft and the missile with elevators 2 and 4 deflected –20 deg are shown in Fig. 18. The force- and moment-coefficient increments are shown in Fig. 19. The free-stream results are also shown in this figure. The aircraft flow field seems to have little effect on the control effectiveness of the air-to-air missile. The ratio of the carriage force- and moment-coefficient increments to the free-stream values is shown in Table 2. The carriage normal-force and the pitching-moment coefficient increments, which are the only significant force- and moment-increments with this deflection configuration, are within 20 percent of their free-stream values in this highly nonuniform flow field. The pressure-coefficient distribution at the midspan location of elevator 4 is shown in Fig. 20 for both free stream and carriage. Except for differences near the leading edge which are attributable to the large flow angles present from the aircraft, the distributions are very similar.

Conclusions

Navier-Stokes calculations were performed to investigate the changes in control surface effectiveness of a store in the interference flow field of a parent aircraft. Two stores were investigated (AGM-130A and an air-to-air missile) in the F-15E flow field. Free-stream calculations showed good agreement with wind tunnel control surface effectiveness results for both stores. Calculations of control surface effectiveness in the presence of the aircraft indicated that significant changes occur for the AGM-130A in the carriage position on the inboard wing pylon, while only small changes were found for the air-to-air missile mounted on the forward station of the inboard long pylon. Calculations of the aircraft flow field without the stores present showed that the flow was significantly more nonuniform in the vicinity of the forward station of the inboard long pylon. The differences in the results for the two stores is attributed to the fact that a large region of separated flow exists on the leeward side of the AGM-130A deflected flap, while the flow over the air-to-air missile elevator is attached over the range of deflections investigated. The separated flow region is much more sensitive to the changes in the external flow.

This effort investigated the validity of using free-stream control surface effectiveness coefficients

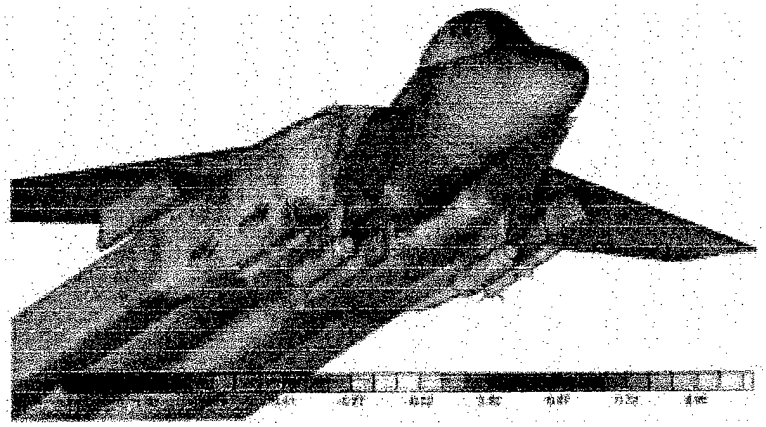

Fig. 18. Pressure coefficient contours for the F-15E with the air-to-air missile at carriage for M = 0.9, α = 0 deg, and $\delta_{2,3}$ = –20 deg.

Table 2. CFD predicted ratio of force- and moment-coefficient increments at the carriage position to the free-stream force- and moment-coefficient increments for the air-to-air missile

		rcx	rcy	rcz	rmx	rmy	rmz
N-S	–10	1.2930	0.9204	1.1890	6.50	1.1870	0.4080
N-S	–20	1.0820	0.7552	1.0611	2.24	1.0620	1.4670

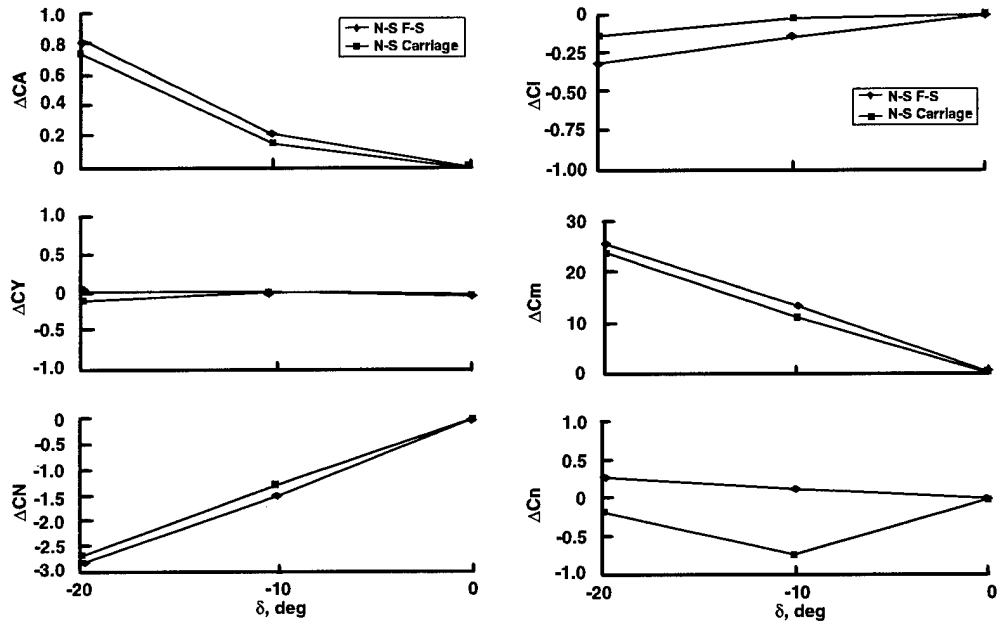

Fig. 19. Force and moment incremental coefficients for the air-to-air missile at carriage and in free stream for M = 0.9.

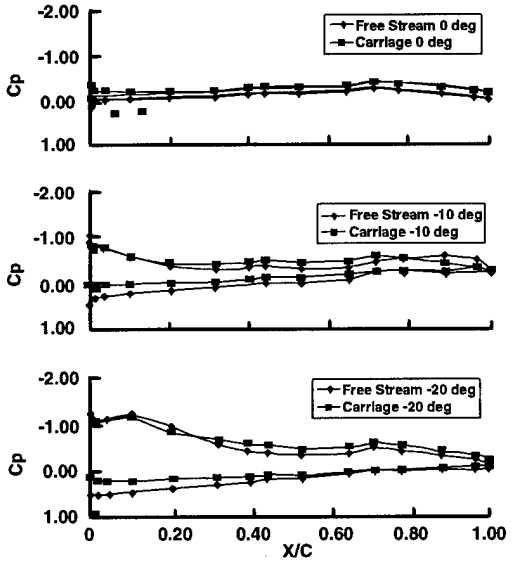

Fig. 20. Pressure coefficient distributions on the deflected elevator (4) of the air-to-air missile for M = 0.9.

when computing the trajectory of a maneuvering store in the nonuniform flow field of a parent aircraft. Two distinct classes of stores were investigated: a store with a wing/flap arrangement (AGM-130A) and a store with an all-moving aft control surface (air-to-air missile). The study indicates that for stores with little or no separation of the flow along the control surface, the use of free-stream control surface effectiveness coefficients is a reasonable approximation. When significant separation of the flow is present, the assumption is questionable.

References

1. Fox, J. H., Donegan, T. L., Jacocks, J. L., and Nichols, R. H. "Computed Euler Flow Field for a Transonic Aircraft with Stores," *Journal of Aircraft*, Vol. 28, No. 6, June 1991, pp. 389-396.

2. Donegan, T. L. and Fox, J. H. "Analysis of Store Trajectories from Tactical Fighter Aircraft," AIAA-91-0183, January 1991.

3. Nichols, R. H., Jacocks, J. L., and Rist, M. J. "Calculation of the Carriage Loads of Tandem Stores on a Fighter Aircraft," AIAA-92-0283, January 1992.

4. Benek, J. A., Buning, P. G., and Steger, J. L. "A 3-D Chimera Grid Embedding Technique," AIAA-85-1523, July 1985.

5. Suhs, N. E. and Tramel, R. W. "PEGSUS 4.0 User's Manual," AEDC-TR-91-8, October 1991.

6. Beam, R. and Warming, R. F. "An Implicit Finite-Difference Algorithm for Hyperbolic Systems in Conservation-Law Form," *Journal of Computational Physics*, Vol. 22, September 1976, pp. 87-110.

7. Pulliam, T. H. and Steger, J. L. "Implicit Finite-Difference Simulations of Three-Dimensional Compressible Flow," *AIAA Journal*, Vol. 18, No. 2, February 1980, pp. 156-169.

8. Benek, J. A., Donegan, T. L., and Suhs, N. E. "Extended Chimera Embedding Scheme with Application to Viscous Flows," AIAA-87-1126, July 1987.

9. Baldwin, B. S. and Lomax, H. "Thin Layer Approximation and Algebraic Model for Separated Turbulent Flows," AIAA-78-257, January 1978.

10. Dietz, W. E. "General Approach to Calculating Forces and Moments on Overset Grid Configurations," Proceedings of the Second Overset Composite Grid and Solution Technology Symposium, October 1994.

REPORT DOCUMENTATION PAGE

Form Approved
OMB No. 0704-0188

1. AGENCY USE ONLY *(Leave blank)*	2. REPORT DATE	3. REPORT TYPE AND DATES COVERED
	June 1997	Technical Society Paper

4. TITLE AND SUBTITLE
Assessment of Store Control Surface Effectiveness in a Non-Uniform Aircraft Flow Field
AIAA Paper No. 97-2200

5. FUNDING NUMBERS

6. AUTHOR(S)
R. H. Nichols and S. B. Evans

7. PERFORMING ORGANIZATION NAME(S) AND ADDRESS(ES)
Sverdrup Technology, Inc./AEDC Group
740 Fourth Street
Arnold Air Force Base, Tennessee 37389-6001

8. PERFORMING ORGANIZATION REPORT NUMBER

9. SPONSORING/MONITORING AGENCY NAME(S) AND ADDRESS(ES)
Arnold Engineering Development
Anrold AFB, TN 37389

10. SPONSORING/MONITORING AGENCY REPORT NUMBER

11. SUPPLEMENTARY NOTES
15th AIAA Applied Aerodynamics Conference, Atlanta, GA, June 23-25, 1997

12a. DISTRIBUTION AVAILABILITY STATEMENT
Approved for public release; distribution unlimited.

12b. DISTRIBUTION CODE
A

13. ABSTRACT *(Maximum 200 words)*

Comparisons of the control effectiveness for two stores in free stream and in the flow field of a parent aircraft have been performed using compu-tational fluid dynamics (CFD). The computations were performed to assess the changes in control surface effectiveness of the store due to the highly nonlinear flow field of the parent aircraft at tran-sonic speeds. The Navier-Stokes equations were solved using an algebraic turbulence model for an extended range air-to-ground missile (AGM-130A) mounted on the wing pylon of an F-15E aircraft and for an air-to-air missile mounted on the forward sta-tion of the inboard pylon of an F-15E aircraft. Free-stream calculations showed good agreement with wind tunnel control surface effectiveness results for both stores. Calculations of control surface effectiveness in the aircraft flow field indicate significant changes occur for the AGM-130A missile while the air-to-air missile showed very little effect. This is attributed to the fact that a large region of separated flow occurs on the lee side of the deflected flap of the AGM-130A while the flow over the air-to-air missile deflected elevator is attached.

14. SUBJECT TERMS	15. NUMBER OF PAGES
control effectiveness, stores, CFD	13
	16. PRICE CODE

17. SECURITY CLASSIFICATION OF REPORT	18. SECURITY CLASSIFICATION OF THIS PAGE	19. SECURITY CLASSIFICATION OF ABSTRACT	20. LIMITATION OF ABSTRACT
Unclassified	Unclassified	Unclassified	UL